

Model of transverse electrical conductivity of metal matrix composites above liquid nitrogen temperatures

Part 1 Regular arrays of fibres

JACQUES E. SCHOUTENS*

MMCIAC, Kaman Tempo, 816 State Street, Santa Barbara, California 93102, USA

FRANCESCO S. ROIG

College of Creative Studies, University of California, Santa Barbara, California 93106, USA

The present theories of transverse electrical conductivity of metal matrix composites (MMCs) containing nonconducting continuous cylindrical fibres are inadequate to predict experimental measurements. In this paper, we present a model of transverse electrical conductivity that predicts experimental data reasonably well for the case of an MMC material reinforced with nonconducting or poorly conducting continuous fibres. It is based on the concept that transverse conductivity consists of two contributions: the electrical resistivity of the bulk material modified by periodic variations in the bulk cross-section due to the presence of nonconducting fibres; and a disturbance in electron transport due to nonuniformity in the electric field, caused by the presence of the fibres, that extends some distance away from and all around the fibres. To calculate this nonuniformity, we use the well-known solution of the potential field for a conducting cylinder in a uniform electric field and invert it so that it becomes a problem of nonconducting filaments in a conducting matrix. This gives a value of the transverse electrical resistivity for boron/aluminium (B/Al) containing 60 vol% fibre in nearly exact agreement with experimental data. The theory is compared to a modified capacitance model developed by Keller [1] for dielectric materials. The model discussed in this paper does not predict the transverse electrical resistivity of MMCs reinforced with very small-diameter fibres (Gr/Al, Al₂O₃, etc.) where the fibres are randomly distributed in a plane normal to their longitudinal axis. This problem will be discussed in a companion paper.

1. Introduction

A number of transverse electrical conduction (resistivity) models for *in situ* and metal matrix composites (MMCs) containing nonconducting continuous fibres have been proposed. All of these models are macroscopic. An excellent review of these models was recently given by Jenkins [2]. We will briefly discuss some of the more important models. Liebmann and Miller [3] proposed the following equation to calculate the electrical resistivity of InSb-Sb eutectic alloys

$$\frac{1}{\rho_{\perp}} = \frac{1}{\rho_{\text{InSB}}} (1 - v^{1/2}) + \left[\rho_{\text{InSB}} \left(\frac{1 + v^{1/2}}{v^{1/2}} \right) + \rho_{\text{Sb}} \right]^{-1} \quad (1)$$

where $v = V_f/(1 + V_f)$, where V_f is the fibre volume fraction of the composite; ρ_{\perp} is the transverse electrical resistivity; and ρ_{InSB} and ρ_{Sb} are the resistivities of indium antimonide and antimony, respectively. This theory explains the conductivity of InSB-Sb eutectic alloys by means of a simple electric analogue of the

eutectic structure. Applying this equation to MMCs where the fibre resistivity is considered much greater than the resistivity of the bulk matrix, Equation 1 reduces to

$$\rho_{\perp} \approx \rho_0 (1 - v^{1/2})^{-1} \quad (2)$$

where ρ_0 is the matrix or bulk resistivity.

There are three theories based on the calculation of dielectric constants of a composite consisting of parallel fibres in a matrix with a different dielectric constant. These theories have been used to calculate the transverse electrical resistivity of composite materials, including MMCs. The reasoning behind this approach was that the dielectric constant can be replaced by the corresponding expressions for electrical conductivity. The theory of Rayleigh [4], which is based on a dilute suspension for a random dispersion of spheres, gives

$$\frac{\sigma_{\perp} - \sigma_0}{\sigma_{\perp} + \sigma_0} = \frac{\sigma_f - \sigma_0}{\sigma_f + \sigma_0} V_f \quad (3)$$

where σ_{\perp} is the transverse conductivity of the

* Author to whom correspondence should be addressed.

TABLE I Comparison between model predictions and measured transverse electrical resistivity of B/Al

Model and equation	Volume fraction							
	0.15		0.223		0.35		0.60	
	Calculated* ($\mu\Omega$ cm)	Measured [10] [†] ($\mu\Omega$ cm)	Calculated ($\mu\Omega$ cm)	Measured [10] ($\mu\Omega$ cm)	Calculated ($\mu\Omega$ cm)	Measured [10] ($\mu\Omega$ cm)	Calculated ($\mu\Omega$ cm)	Measured [9] ($\mu\Omega$ cm)
Liebmann and Miller [3], Equation 2	5.20	4.6 (0.89) [‡]	5.79	5.45 (0.94)	6.76	6.91 (1.02)	8.56	35.5 (4.14)
Rayleigh [4], Equation 4	4.49	4.6 (1.02)	5.23	5.45 (1.04)	6.90	6.91 (1.00)	13.28	35.5 (2.67)
Davies [5], Equation 7	4.74	4.6 (0.97)	5.99	5.45 (0.91)	11.07	6.91 (0.62)	-16.75 [§]	35.5 (-)
Keller [1], Equation 8	3.84	4.6 (1.20)	4.87	5.45 (1.12)	6.97	6.91 (0.99)	15.21	35.5 (2.33)

*In these calculations, we assumed $\rho_0 = 3.32 \mu\Omega$ cm for 6061 Al ribbons [9].

[†]The data from Yatsenko [10] were corrected to have a matrix resistivity of $3.32 \mu\Omega$ cm.

[‡]The numbers in parentheses are the factors by which the measured values are larger, equal, or smaller than the predicted values.

[§]When applied to MMC, Davies' theory ($\sigma_f \ll \sigma_0$) gives negative values for ρ_{\perp} when $V_f > 0.5$.

composite; σ_f and σ_0 are the fibre and matrix conductivities, respectively; and V_f is the fibre volume fraction. For graphite/aluminium (Gr/Al), alumina/aluminium, boron/aluminium (B/Al), and silicon carbide/aluminium (SiC/Al), $\sigma_f \ll \sigma_0$, so that Equation 3 reduces to

$$\rho_{\perp} = \rho_0 \left(\frac{1 + V_f}{1 - V_f} \right) \quad (4)$$

Another theory due to Davies [5] gives the following implicit relation. This model is known as an effective medium theory, which is equivalent to the coherent potential approximation in the theory of disordered alloys or to the T-matrix approximation in scattering theory, and to a random array of parallel cylinders.

$$\sigma_{\perp} = \sigma_0 + 2V_f\sigma_{\perp} \left(\frac{\sigma_f - \sigma_0}{\sigma_{\perp} + \sigma_f} \right) \quad (5)$$

which leads to a quadratic equation in σ_{\perp} with the following positive solution

$$\sigma_{\perp} = -\frac{1}{2}(1 - 2V_f)(\sigma_f - \sigma_0) \times \left(1 + \left\{ 1 - \frac{4\sigma_0\sigma_f}{[(1 - 2V_f)(\sigma_f - \sigma_0)]^2} \right\}^{1/2} \right) \quad (6)$$

and when $\sigma_f \ll \sigma_0$ is considered, Equation 6 reduces to

$$\rho_{\perp} = \rho_0(1 - 2V_f)^{-1} \quad (7)$$

The theory of Peterson and Hermans [6] is essentially the same as that of Davies and gives the same result.

Keller [1] and Keller and Sachs [7] proposed another theory for an array of nonconducting cylinders in a conducting medium, given by

$$\rho_{\perp} = \rho_0 \frac{2}{(v - 2)^{1/2}} \tan^{-1} \left(\frac{v}{v - 2} \right)^{1/2} \quad (8)$$

where $v = (\pi/V_f)^{1/2}$. This has the disadvantage of giving $\rho_{\perp} = 0$ at $V_f = 0$, instead of $\rho_{\perp} = \rho_0$, and becomes singular at $V_f = \pi/4$. This expression was shown by Crank [8] to be equivalent to an effective

diffusion coefficient in cases of diffusion perpendicular to an array of parallel circular obstructions.

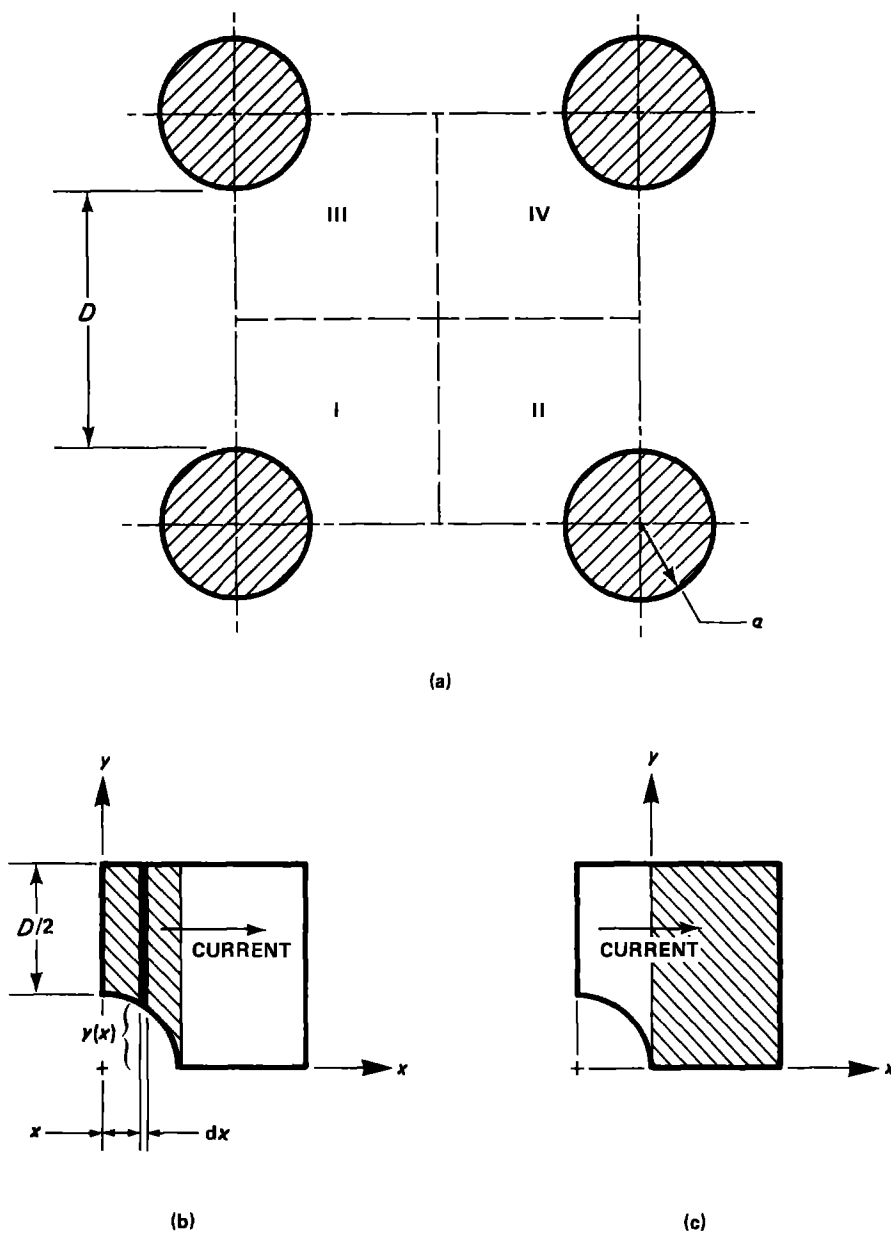
Calculations using the above theories give results shown in Table I for a B/Al composite. These results are compared to measurements made by Abukay *et al.* [9] and Yatsenko [10]. The numbers in parentheses are the factors by which the measured values are larger, equal, or smaller than those predicted by the models and equations indicated. Note that for volume fractions up to 35% the models give fairly good predictions. This is expected because the models in question are known as dilute suspension models.

In this paper, we present a model of transverse electrical conductivity of *in situ* composites and MMCs at temperatures above about that of liquid nitrogen. Below that temperature threshold, and for very small-diameter fibres such as graphite fibres in an aluminium matrix and *in situ* composites, electron scattering begins to contribute additional resistivity to the composite which cannot be calculated by macroscopic models, as shown by Roig and Schoutens [11] for longitudinal conductivity.

2. Theory

Table I shows that present theoretical treatments of the transverse electrical conductivity of MMCs predict values that are a factor of about 2 to 4 below measured values for high volume fraction B/Al, and other data to be discussed below. The measured resistivities for a volume fraction of 0.6 are the work of different authors [9] compared to those for volume fractions of 0.15, 0.223, and 0.35 [10]. This might account for the disagreement of the theoretical predictions for the high volume fraction, and also because all measurements were clearly not on the same samples. One hypothesis is that the transverse electrical resistivity in an MMC is the sum of two contributions: the first is due to the fact that the electrical resistivity varies periodically with the position of the fibre in the matrix; and the second comes from disturbances in the electron drift as they proceed transversely across the

Figure 1 Cell model used in calculating periodic variations in bulk conductivity: (a) cell, (b) variable cross-section, (c) constant cross-section.



array of fibres. In mathematical terms,

$$\rho_{\perp} = \rho_0 f(V_f) [1 + C(V_f, \alpha)] \quad (9)$$

where $f(V_f)$ is a resistivity function dependent on the shape and volume fraction of fibres, and $C(V_f, \alpha)$ is a function that accounts for the fact that the transverse electric field in the bulk is nonuniform due to the presence of fibres. Moreover, from classical electrodynamics, such a nonuniformity has a range α , beyond which it is again uniform.

2.1. Derivation of the resistivity function

Fig. 1 shows a square cell of composite material with a fibre of radius a at each corner and each fibre separated by a distance D as shown. We conceptually divide the cell into four regions, marked I to IV, and proceed to calculate the resistivity of region I of unit depth in the direction of the fibres. It is assumed that an electric field is applied in a direction perpendicular to the fibres and along the horizontal axis joining two fibres, thereby creating a current as shown. In region I of the cell, the elemental resistance

dR near the fibre is

$$dR = \rho_0 \frac{dx}{A(x)} \quad (10)$$

where dx is the infinitesimal matrix thickness normal to the current as shown in Fig. 1b, and $A(x)$ is the variable cross-section in that region when $0 \leq x \leq a$, or

$$A(x) = \left[a + \frac{D}{2} - Y(x) \right] L \quad (11)$$

where L is the distance along the fibre, and $Y(x) = (a^2 - x^2)^{1/2}$. Substituting Equation 11 into Equation 10 and integrating gives

$$R_1 = \frac{\rho_0}{L} \int_0^a \frac{dx}{a + (D/2) - (a^2 - x^2)^{1/2}} \quad (12)$$

The integration of Equation 12 is carried out by letting $1 + D/2a = \alpha_0$ and using successively $w = x/a$ and $w = \sin \theta$. After integration, this gives

$$R_1 = \frac{\rho_0}{L} \left[-\frac{\pi}{2} + \frac{2\alpha_0}{(\alpha_0^2 - 1)^{1/2}} \tan^{-1} \left(\frac{\alpha_0 + 1}{\alpha_0 - 1} \right)^{1/2} \right] \quad (13)$$

The resistance of the shaded region shown in Fig. 1c is

$$R_2 = \rho_0 \frac{D/2}{(a + D/2)L} = \frac{\rho_0}{L} \left(1 - \frac{1}{\alpha_0}\right) \quad (14)$$

and the total resistance of region I is $R_1 + R_2$, or

$$R_c = \frac{\rho_0}{L} \left[\left(1 - \frac{1}{\alpha_0} - \frac{\pi}{2}\right) + \frac{2\alpha_0}{(\alpha_0^2 - 1)^{1/2}} \tan^{-1} \left(\frac{\alpha_0 + 1}{\alpha_0 - 1} \right)^{1/2} \right] \quad (15)$$

For convenience in computing R in the limit, we set $\beta = 1/\alpha_0$; then, Equation 15 becomes

$$R_c = R_0 \left[\left(1 - \beta - \frac{\pi}{2}\right) + \frac{2}{(1 - \beta^2)^{1/2}} \tan^{-1} \left(\frac{1 + \beta}{1 - \beta} \right)^{1/2} \right] \quad (16)$$

where $R_0 = \rho_0/L$. When the fibre radius approaches zero ($a \rightarrow 0$), $\beta \rightarrow 0$ and $R_c = R_0$, as it should. The second term in the bracket is greater than $\pi/2$ for $\beta < 1$ and, consequently, the term in the bracket is always positive, giving R always positive. Moreover, as the space between fibres approaches zero ($D \rightarrow 0$), $\beta \rightarrow 1$ and $R \rightarrow \infty$, meaning that when the fibres are in contact, the composite resistance is at least that of the fibres, which can be quite high for MMCs containing graphite or boron fibres.

Now, resistance of regions I and II is $2R_c$, and the resistance of regions I to IV is then the total resistance given by

$$\frac{1}{R_T} = \frac{1}{2R_c} + \frac{1}{2R_c} = \frac{1}{R_c} \quad (17)$$

Thus, the total resistance of the cell is given by Equation 16.

Equation 16 can be converted to electrical resistivity in the following manner. The resistance of a sample of composite with respect to the resistance of a sample of bulk material without fibres ($V_f = 0$) is

$$\frac{R(\beta)}{R_0(0)} = \frac{R_c}{R_0} = f(\beta) \quad (18)$$

where

$$f(\beta) = \left[\left(1 - \beta - \frac{\pi}{2}\right) + \frac{2}{(1 - \beta^2)^{1/2}} \tan^{-1} \left(\frac{1 + \beta}{1 - \beta} \right)^{1/2} \right] \quad (19)$$

and for the bulk, $R_0 = \rho_0 l/A = \rho_0(D + 2a)/L(D + 2a) = \rho_0/L$, and for the composite, $R_c = \rho_c l/A = \rho_c(D + 2a)/L(D + 2a) = \rho_c/L$, where ρ_c is the composite resistivity. Substituting these values in Equation 18 yields

$$\frac{\rho_c}{\rho_0} = f(\beta). \quad (20)$$

Equation 20 is the transverse electrical resistivity of an MMC material due to periodic variations in the bulk cross-section in the direction of the current due to the

TABLE II Values of V_f as a function of β from Equation 24

V_f	β
0.0	0.000
0.1	0.357
0.2	0.505
0.3	0.618
0.4	0.714
0.5	0.798
0.6	0.874
0.7	0.944
0.785	1.000

presence of fibre boundaries, assuming the electric field remains uniform.

Now, a relationship between β and V_f must be found so that the above derivation has practical utility. From Fig. 1a, we note that the volume of fibre in the cell is

$$v_f = \pi a^2 L \quad (21)$$

and the total volume of the cell is

$$v_T = (D + 2a)^2 L \quad (22)$$

so that the fibre volume fraction is

$$V_f = \frac{v_f}{v_T} = \frac{\pi}{4} \left(\frac{1}{1 + D/2a} \right)^2 \quad (23)$$

where L is the length of the fibre. Recalling that $\alpha_0 = 1 + D/2a$ and substituting into Equation 23 gives $V_f = \pi/(4\alpha_0^2)$ and, using the definition of $\beta = 1/\alpha_0$, we obtain

$$V_f = \frac{\pi}{4} \beta^2. \quad (24)$$

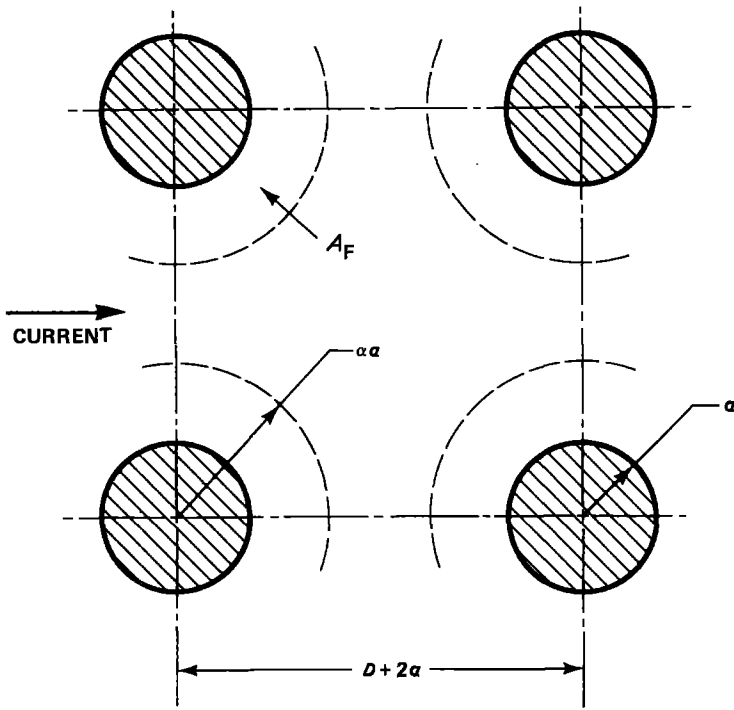
Thus, Equation 20 can be written as

$$\rho_c = \rho_0 f(V_f) \quad (25)$$

where V_f is substituted for β in Equation 19 according to Equation 24. Table II gives values of V_f as a function of β , and Table III gives the values of the resistivity function $f(V_f)$ as a function of V_f . We see in Table III that $f(0) = 1$, as it should, and $f(V_f) \rightarrow \infty$ for $V_f \rightarrow \pi/4$. For 60 vol % B/6061 Al composite, we note that according to Equation 25, the transverse electrical conductivity is $\rho_c = \rho_0 f(V_f) = 3.32(3.977) = 13.204 \mu\Omega \text{ cm}$, or about the same value as that given by Rayleigh's Equation 4 [4] shown in Table I, which is a factor of about 2.7 below the value measured by Abukay *et al.* [9].

TABLE III Values of the resistivity function $f(V_f)$ as a function of V_f

V_f	$f(V_f)$
0.0	1.000
0.1	1.144
0.2	1.357
0.3	1.657
0.4	2.092
0.5	2.770
0.6	3.977
0.7	6.993
0.785	∞



2.2. Derivation of the correction function

An applied uniform electric field causes electrons to drift uniformly through a near-ideal metal in the absence of obstacles. In the presence of obstacles such as grain boundaries, dislocations, and defects, the electric field is locally nonuniform. When the metal is reinforced by nonconducting cylindrical fibres placed perpendicularly to the uniform electric field, that field becomes locally and periodically nonuniform. Thus, the electrons drift along periodically varying field lines. The field lines in the immediate neighbourhood of the fibre terminate at the fibre/matrix interface – approximately normal if the fibre position is an empty cavity, or at an angle proportional to the dielectric constant if the cavity is filled with a dielectric fibre. In the following analysis, we will assume that the matrix is a near-ideal metal so that the electric field in the absence of obstacles is uniform and that the cavity is empty. (Inside a perfect conductor, there cannot be electric fields.) Consequently, the dielectric properties of the fibre are not considered. In essence, then, this is the inverted problem of a conducting cylinder in a uniform electric field in empty space. From classical electrodynamics [12], the scalar potential at a point $P(r, \theta)$ in the neighbourhood outside the fibre is given in cylindrical coordinates by

$$\phi = -E_0 r \cos \theta \left(1 - \frac{a^2}{r^2} \right) \quad (26)$$

where E_0 is the uniform electric field, a is the fibre or cavity radius, and r and θ are the polar coordinates of the point P where the field components are determined. The radial and angular components of the electric field are obtained from the scalar potential by $\vec{E} = -\nabla\phi$ or

$$E_r = -\frac{\partial\phi}{\partial r} = E_0 \cos \theta \left(1 + \frac{a^2}{r^2} \right) \quad (27)$$

$$E_\theta = -\frac{1}{r} \frac{\partial\phi}{\partial\theta} = -E_0 \sin \theta \left\{ 1 - \frac{a^2}{r^2} \right\} \quad (28)$$

The total field at $P(r, \theta)$ is

$$E_T^2 = E_r^2 + E_\theta^2 \quad (29)$$

and to find the average value over the entire space from $a \leq r \leq \alpha a$ and for $0 \leq \theta \leq 2\pi$, where α is a dimensionless range parameter, we integrate both sides of Equation 29 as follows

$$\int_0^{2\pi} \int_a^{\alpha a} E_T^2 r \, dr \, d\theta = \int_0^{2\pi} \int_a^{\alpha a} (E_r^2 + E_\theta^2) r \, dr \, d\theta \quad (30)$$

Substituting Equations 27 and 28 into Equation 30 and integrating gives

$$\langle E_T^2 \rangle = E_0^2 \left(1 + \frac{1}{\alpha^2} \right) \quad (31)$$

Equation 31 shows that the total electric field calculated in this manner consists of two components, the uniform field term plus a second order term that depends on the range parameter α . It is this second order term that, on average, accounts for the effects of nonuniformity upon electrons in the electric field in the neighbourhood of a fibre. Therefore, we can write

$$\frac{\delta E_0}{E_0} \simeq \frac{1}{\alpha} \quad (32)$$

where E_0 is the uniform electric field, and δE_0 is the perturbation of that field. The electric field is nonuniform around the fibre out to a range $\alpha a \lesssim 3a$, as can be seen in electric field maps for this classical problem.

The range αa of this nonuniform field does not occupy the entire cell of interest but only a region of area A_F ; as shown in Fig. 2. For high fibre volume fraction, the areas are expected to overlap. This overlap problem is not treated in the simple model discussed in this paper. Consequently, there is a region in the cell

where the electric field is uniform and other regions where it is not uniform. Letting the area of non-uniform field be A_F for $\alpha \lesssim 3$ and letting A_c be the area of the cell, as shown in Fig. 2, then the correction function is taken to be

$$C(V_f, \alpha) = \frac{\delta E_0}{E_0} \left(\frac{A_F}{A_c} \right) = \frac{1}{\alpha} \frac{A_F}{A_c} \quad (33)$$

and we will see that this assumption can fit the data, and from Fig. 2, $A_c = (D + 2a)^2$ and $A_F = \pi a^2(\alpha^2 - 1)$, so that Equation 33 becomes

$$C(V_f, \alpha) = \left\{ \frac{\alpha^2 - 1}{\alpha} \right\} V_f \quad (34)$$

where Equation 23 was used. This correction factor has the correct form since for $V_f = 0$, $C(0, \alpha) = 0$. Therefore, in the absence of fibres, there are no non-uniformities in the electric field.

2.3. Complete transverse resistivity equation

Returning to Equation 9, we have

$$\rho_{\perp} = \rho_0 f(V_f) [1 + C(V_f, \alpha)]$$

and substituting Equation 34 gives

$$\rho_{\perp} = \rho_0 f(V_f) \left[1 + \left(\frac{\alpha^2 - 1}{\alpha} \right) V_f \right] \quad (35)$$

where $f(V_f)$ is given by Equation 16. Equation 35 gives $\rho_{\perp} = \rho_0$ for $V_f = 0$ since $f(0) = 1$, and the second term vanishes at $V_f = 0$. Moreover, $\rho_{\perp} \rightarrow \infty$ when $V_f \rightarrow \pi/4$ since $f(V_f \rightarrow \pi/4) \rightarrow \infty$, which corresponds to the fibres being in actual contact with one another in the matrix. It should be emphasized that Equation 35 applies only for the case where the fibres in the matrix form a regular array, either square or quasi-square. This is a consequence of the fabrication process employed in large-diameter fibre reinforced MMC materials such as B/Al. For the case of very small-diameter fibres, of the order of a few tens of micrometres, the distribution of fibre cross-sections in a plane normal to the fibre axis is nearly random. The electrical resistivity for such cases requires a different theory, which is discussed elsewhere [13].

3. Discussion

Returning to Equation 35 and using the value $\alpha = 3$, there results

$$\rho_{\perp} = \rho_0 f(V_f) (1 + 2.667 V_f) \quad (36)$$

The predicted values of the transverse electrical conductivity of MMCs are given in Table IV and plotted in Fig. 3 as a function of V_f . The predicted value of ρ_{\perp} is seen to pass close to the datum point for 60 vol % B/Al composite. Also shown are three data points, joined by a line of short dashes, from the work of Yatsenko [10]. The data published by Yatsenko were for a matrix resistivity of $3.21 \mu\Omega \text{ cm}$. Consequently, these data were scaled in Fig. 3 by the factor $3.32/3.21 = 1.036$ to make comparisons meaningful. As mentioned before and shown in Table I, the theories discussed in the introduction give predictions in good agreement with Yatsenko's data. The agreement with the datum point for 60 vol % B/Al appears excellent:

$34.33 \mu\Omega \text{ cm}$ predicted compared to $35.5 \mu\Omega \text{ cm}$ measured, or a difference of 3.3%. Such an agreement may mean the following, aside from being fortuitous. At high volume fraction, the electric field intensity around fibres increases while the region of field uniformity between fibres decreases, resulting in a net increase in the composite resistance. As the fibre distance increases (lower values of V_f), this model seems to overpredict the field effect. We should recall that the model is rather simplistic, and a more detailed description might be in order. It turns out that considering the field contributions from all fibres surrounding one fibre in a cell by assuming superposition of field does not improve predictions very much at low values of V_f [14].

Another group of data for Gr/Al and Gr/Mg [15] is shown in Fig. 3. An examination of photomicrographs of such composite materials reveals very irregular, almost random fibre distributions in a plane perpendicular to the fibre axis. At low fibre volume fraction, these photomicrographs show numerous filaments in actual physical contact forming "strings" separated by irregular regions of matrix materials. Under such conditions, one would thus expect, on intuitive grounds, that the current follows tortuous paths with statistically varying resistivity. At high volume fraction, the number of filaments in physical contact is so large as to isolate islands of matrix material. Consequently, one would expect the transverse conductivity for these materials to be higher than that shown by the present model or the data for B/Al. Aside from matrix resistivity due to periodic variation in the matrix cross-section in between fibres and the added electric field effect discussed, it is likely that there is a capacitance effect in the immediate neighbourhood of closely spaced fibres. To test this hypothesis, we have modified Keller's theory [1], which is based on the capacitance that exists between two fibres along the direction of the current for conducting fibres embedded in a dielectric. Keller then inverted the result of his analysis to account for resistivity transverse to nonconducting cylinders embedded in a conducting matrix. This resulted in Equation 8 discussed above. If we neglect the electric field non-uniformity at $0.1 \lesssim V_f \lesssim 0.4$ and consider only resistivity variations and capacitance effects, the modified Keller theory can be written as

$$\rho_{\perp} = \rho_0 [f(V_f) + C(V_f)] \quad (37)$$

TABLE IV Values of ρ_{\perp} predicted from Equation 36

V_f	ρ_{\perp} ($\mu\Omega \text{ cm}$)
0.0	3.32*
0.1	4.81
0.2	6.91
0.3	9.90
0.4	14.35
0.5	21.46
0.6	34.33
0.7	66.56
0.785	∞

* $\rho_0 = 3.32 \mu\Omega \text{ cm}$ for 6061 Al [9].

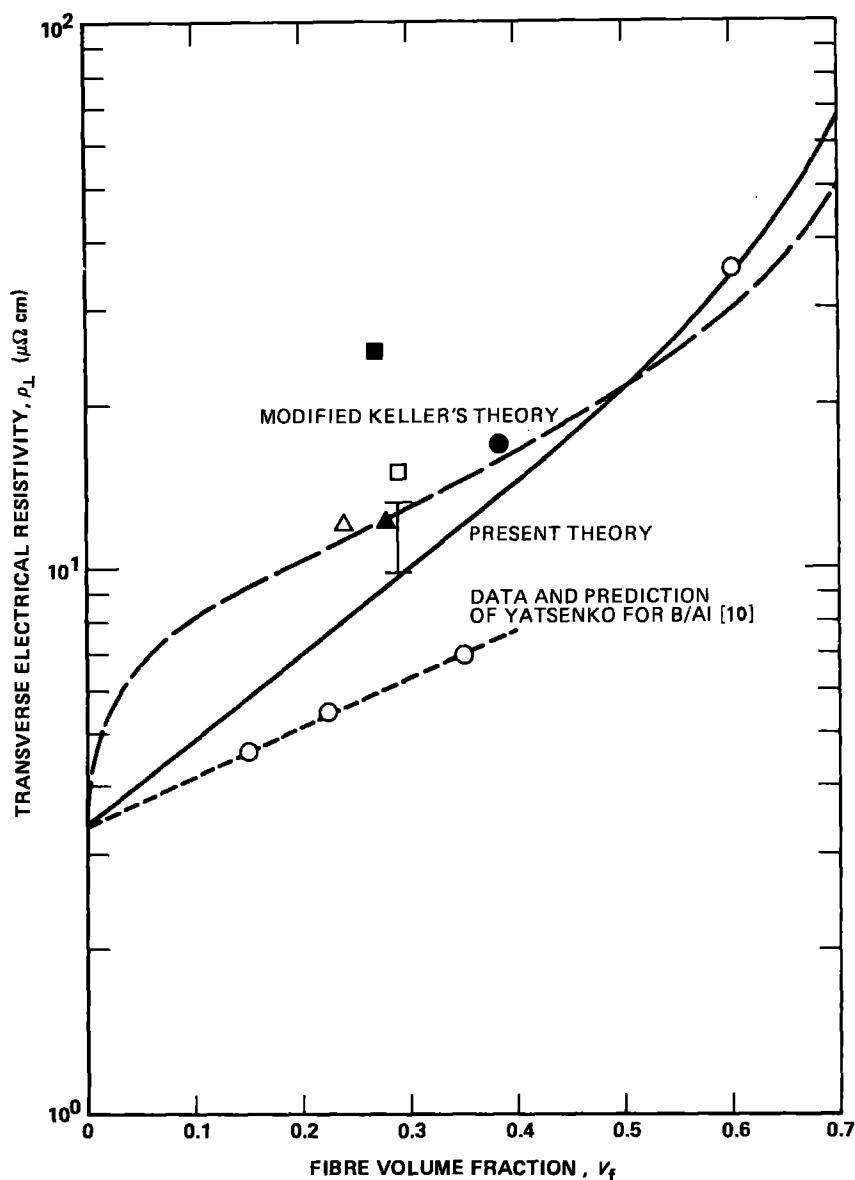


Figure 3 Plot of the present theory and Keller's original and modified theories, and comparison with some experimental data. Room temperature data: (O) B/6061 Al; (□) 29 vol % Gr/201 Al, with 0.004 in. 2024 Al cladding, liquid nitrogen quenched 3 times; (Δ) 24 vol % Gr/201 Al, with 0.004 in. 2024 Al cladding, liquid nitrogen quenched 3 times; (●) 38.5 vol % Gr/AZ31B Mg; (■) 27 vol % Gr/AZ31B Mg; (▲) 27.75 vol % Gr/201 Al, with 0.002 in. aluminium cladding; (I) 29 vol % Gr/201 Al, with 0.002 in. aluminium cladding.

where $f(V_f)$ is given by Equation 19, and

$$C(V_f) = \frac{2}{(v-2)^{1/2}} \tan^{-1} \left(\frac{v}{v-2} \right)^{1/2} \quad (38)$$

where $v = (\pi/V_f)^{1/2}$. The predictions from Equation 37 are shown in Fig. 3 as a line of long dashes that passes through the group of Gr/Al and Gr/Mg data but falls below the B/Al datum at $V_f = 0.6$. At higher values of V_f , one would expect larger values of ρ_{\perp} for Gr/Al or Gr/Mg than for B/Al, as discussed above. At the present time, some theories are being considered to explain the phenomenon when the fibre arrays are highly irregular or random [13]. Equation 37 has the required behaviour at the limits: when $V_f = 0$, $\rho_{\perp} = \rho_0$, and $\rho_{\perp} \rightarrow \infty$ when $V_f \rightarrow \pi/4$.

The model described in this paper can be scaled to other temperatures (away from room temperature) above about liquid nitrogen temperature and not too close to the matrix melting point. This can be done by using the following scaling rule

$$\rho_{\perp}(T) = \rho_{\perp} \left(\frac{295}{T} \right)^a \quad (39)$$

where ρ_{\perp} is the room temperature resistivity, T is the

temperature of interest in degrees K, and a is a non-integer. From the work of Abukay *et al.* [9], $a = -0.74$ for B/6061 Al.

Acknowledgements

The authors wish to thank Louis A. Gonzalez, Director of the MMCIAC, for his interest and fruitful discussions of this problem and for his support. One author (J.E.S.) is very grateful for the constant spiritual, emotional, and intellectual encouragement given freely to him for over two decades by Mr Daud Peres.

References

1. J. B. KELLER, *J. Appl. Phys.* **34** (1963) 991.
2. T. A. JENKINS, PhD thesis, Clarkson College of Technology, Potsdam, New York (1982).
3. W. K. LIEBMANN and E. A. MILLER, *J. Appl. Phys.* **34** (1963) 2653.
4. J. W. RAYLEIGH, *Phil. Mag.* **34** (1892) 481.
5. W. E. A. DAVIES, *J. Phys.* **D7** (1974) 120.
6. J. M. PETERSON and J. J. HERMANS, *J. Comp. Mater.* **3** (1969) 338.
7. H. B. KELLER and D. SACHS, *J. Appl. Phys.* **35** (1964) 537.
8. J. CRANK, "The Mathematics of Diffusion", 2nd Edn (Clarendon, Oxford, 1975).

9. D. ABUKAY, K. V. RAO and S. ARAJS, *Fibre Sci. Tech.* **10** (1977) 313.
10. M. I. YATSENKO, *Fizika i Khimiya Obrabotki Materialov*, No. 4 (1980) 111.
11. F. S. ROIG and J. E. SCHOUTENS, *J. Mater. Sci.* **21** (1986) 2409.
12. L. D. LANDAU and E. M. LIFSHITZ, "Electrodynamics of Continuous Media" (Pergamon, New York, 1960).
13. J. E. SCHOUTENS, Model of transverse electrical conductivity of metal matrix composites above liquid nitrogen temperatures: Part 2 Irregular arrays of fibres, unpublished data (1985).
14. J. E. SCHOUTENS, unpublished data (1985).
15. H. H. ARMSTRONG and A. M. ELLISON, Lockheed Missiles and Space Co., unpublished data (1979).

*Received 9 December 1985
and accepted 6 May 1986*